Decohesion of Al Grain Boundary by Hydrogen and Liquid Metals: A First-Principles Study

M. Yamaguchi, K. Ebihara, M. Itakura, T. Suzudo, H. Kaburaki

Center for Computational Science and e-systems, Japan Atomic Energy Agency,
Tokai-mura, Ibaraki-ken, 319-1195 JAPAN

The mechanism of hydrogen embrittlement of Al grain boundaries is not well understood for many years. From first-principles calculations, we found that the inner hydrogen in fcc Al can segregate (be trapped) at an Al grain boundary and then decrease its fracture surface energy. On the other hand, we also found that gaseous (outer) hydrogen can not decrease the fracture surface energy of Al by surface adsorption (trappping) from H_2 gas. These results are in good agreement with the experimental facts that the grain boundary embrittlement of Al can be caused by the inner hydrogen but cannot be caused by the outer hydrogen. Our preliminary calculations for Al-(Hg, Ga) systems show that Hg and Ga atoms can also decrease the fracture surface energy by the adsorption on the Al surface. It indicates that both of hydrogen embrittlement and liquid metal (Hg, Ga) embrittlement of Al grain boundaries are caused by the same mechanism: *the reduction of fracture surface energy*. The comparison with the calculations for other metals (Fe, Cu) are also discussed.

1. Introduction

The mechanism of hydrogen embrittlement of metals is not known in detail. This is a very complicated phenomenon because hydrogen interacts with many kinds of defects such as vacancies, voids, dislocations, grain boundaries, interfaces between metal and precipitate, etc. It means that hydrogen can affect both brittle fracture such as cleavage and grain boundary embrittlement, and ductile fracture associated with plastic deformation and dimple formation. In addition, hydrogen can move during fracture even at room temperature especially for iron (Fe) case.

Recently, it has been possible to calculate the trapping energy of hydrogen atoms at a grain boundary (GB) and a fracture surface (FS) in metals from first-principles [1-4]. Using the calculated trapping energies of hydrogen atom, we can estimate the change in the cohesive energy (work of fracture) of GBs of metals. In this paper, we show that many hydrogen atoms can be trapped at an Al grain boundary, and that the cohesive energy of the Al GB can be significantly reduced by the hydrogen trapping. In addition, we show our preliminary calculations for Al-(Hg, Ga) systems, which indicates that liquid metal and hydrogen embrittlement are caused by the same mechanism: the reduction of fracture surface energy by solute atom (H, Hg, Ga) trapping. The calculated results for Al GB are discussed compared with those for Fe and Cu GBs.

2. Calculations

We performed first-principles calculations to simulate the grain boundary decohesion by hydrogen trapping (segregation, adsorption) in ferromagnetic bcc Fe $\Sigma 3(111)$ and non-magnetic fcc Al(Cu) $\Sigma 5(012)$ symmetrical tilt grain boundaries (STGBs). The electronic structure calculations and the structure relaxations by force minimizations are performed using Vienna Ab initio Simulation Package (VASP) with Projector Augmented Wave (PAW) method [5-7]. The cutoff energy for the plane wave basis set is 280 eV, 250 eV, and 273 eV for Fe, Al, and Cu systems, respectively. The Monkhorst Pack k-point mesh is 8x4x1. The Methfessel-Paxton smearing method with 0.1-eV width is used. The PBE exchange-correlation function is used.

Figure 1 shows the unit cells including bcc Σ3(111) and fcc Σ5(012) STGBs. The structures of the two grain boundaries are very close with each other although the crystal structure is different (bcc vs. fcc). Using these unit cells, we calculated the segregation (trapping) energy of hydrogen atoms in the grain boundary ($\Delta E_{GB,total}^{seg}$) and on the fracture surface ($\Delta E_{FS,total}^{seg}$) with varying the trapping density of hydrogen atoms. In this case, the segregation energy is calculated with reference to the solid solution state of hydrogen. From these segregation energies, we calculated the GB cohesive energy ($2\gamma_{int}$) as follows [8],

$$2\gamma_{int} = (2\gamma_s + \Delta E_{FS,total}^{seg} / 2A) - (\gamma_{gb} + \Delta E_{GB,total}^{seg} / A) \tag{1}$$

Here, γ_s and γ_{gb} are the surface and grain boundary energies, respectively. The area of grain boundary plane and fracture surface plane is denoted by A (27.6 Å^2 for Fe, 37.3 Å^2 for Al, and 29.2 Å^2 for Cu). From this equation (1), we can see that the grain boundary cohesive energy ($2\gamma_{int}$) is reduced if the surface segregation energy is larger in negative value than the GB segregation energy.

In the above calculations, we consider the embrittling effect of inner hydrogen, which is incorporated in bulk region of metals and then segregate at grain boundary. When we consider the embrittling effect of gaseous (outer) hydrogen or liquid metal, on the other hand, we calculate the fracture surface adsorption energy ($\Delta E_{FS,total}^{ad}$) of hydrogen from H$_2$ gas or of liquid metal, instead of $\Delta E_{FS,total}^{seg}$. In this case, grain boundary segregation energy ($\Delta E_{GB,total}^{seg}$) is set to zero in Eq. (1) because it is not necessary to consider.
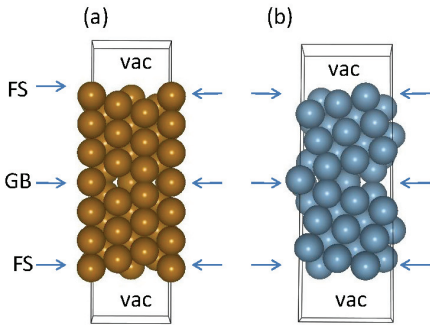

Fig.1: Unit cells for calculations. (a) This cell includes bcc FeΣ3(111) symmetrical tile grain boundary (GB) and (111) fracture surfaces (FSs). (b) This cell includes fcc Al(Cu) Σ5(012) GB and (012) FSs. Vacuum region (vac) is introduced to allow grain boundary sliding along the GB plane.

3. Results and Discussion

3.1 (Fe, Al, Cu)-H systems

At first, we calculated the segregation (trapping) energy of hydrogen atoms when one hydrogen atom is placed at various interstitial atomic sites (octahedral site or tetrahedral site) in the unit cell as shown in Fig. 1. In other words, this is the case for a low trapping density of hydrogen atoms in which the interaction between hydrogen atoms is negligible because the distance between two hydrogen atoms is far enough. This segregation (trapping) energy is calculated with respect to the solid solution state, in which hydrogen atom is at a tetrahedral site in bcc Fe and at an octahedral site in fcc Al(Cu).

The calculated segregation (trapping) energies at various atomic sites are summarized in Fig. 2. The negative value means stable. For Fe case, the largest segregation energy in negative at the FeΣ3(111) STGB is -0.45 eV/atom, while the largest segregation energy in negative at the free surface (FS) is -0.79 eV/atom. It indicates that hydrogen atom stabilizes the iron surface energetically more than the grain boundary. The same trend can be seen in Al and Cu cases, although there are some differences in the size of segregation energies.
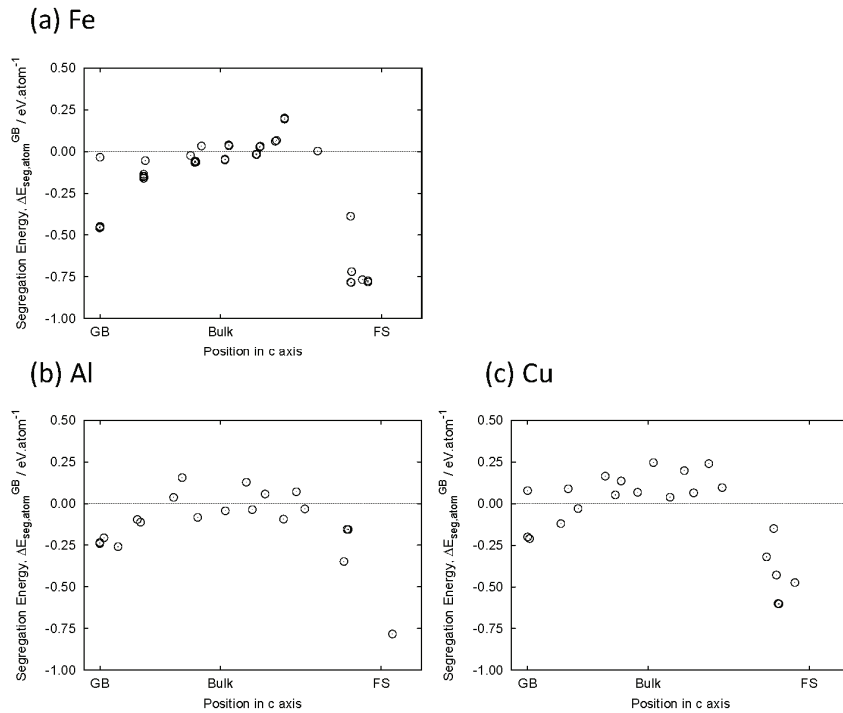
(a) Fe

(b) Al

(c) Cu

Fig.2: Calculated segregation (trapping) energies of hydrogen ($\Delta E_{seg,atom}^{GB}$) when one hydrogen atom is placed at various sites in the cell as shown in Fig.1. GB indicates "grain boundary" and FS "fracture surface". (a) Fe, (b) Al, (c) Cu. These energies are calculated with reference to the solid solution state of hydrogen.

Fig. 3 shows the comparison in energy among the four states. The calculated solid solution energies are in good agreement with experimental data. The GB-trapped (GB-segregated) hydrogen atoms have an embrittling potency if the surface segregation energy is larger in negative than the GB segregation energy, because this energy difference can reduce the cohesive energy of grain boundary as stated above using Eq. (1). From this figure, we can see that the GB-trapped hydrogen has an appreciable size of embrittling potency for all three metals (Fe, Al, and Cu). On the other hand, H_2 gas has an embrittling potency for Fe and Cu cases, but not for Al case. This is in good agreement with the experimental fact that Al does not show H_2 gas embrittlement even under the 85MPa gaseous hydrogen condition [9].
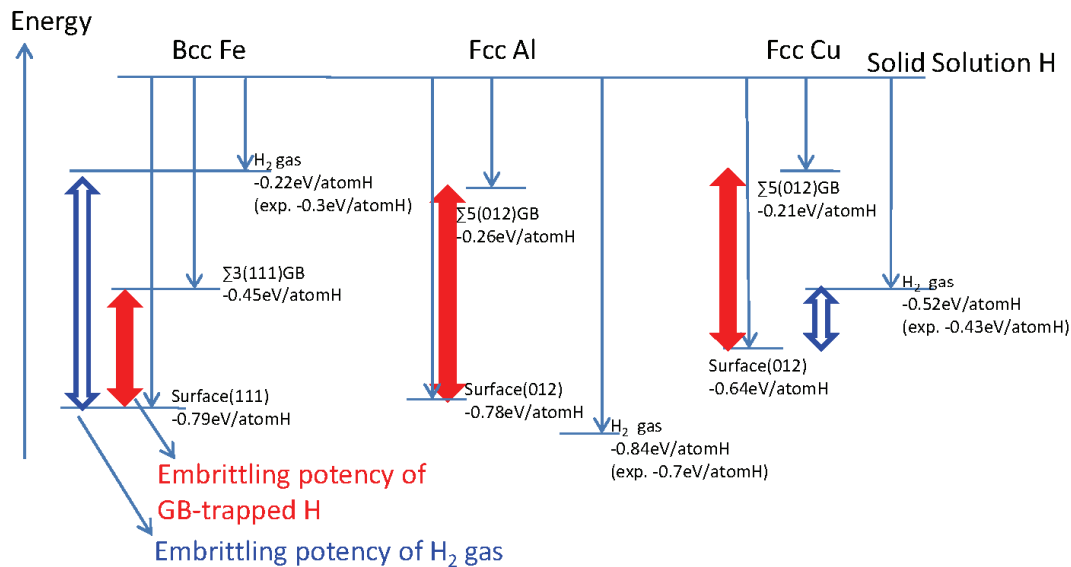

Fig. 3: The comparison in energy among four states, (i) solid solution, (ii) H_2 gas, (iii) grain boundary (GB) segregation, and (iv) surface segregation, in a low segregation concentration case.

Secondly, we calculated the GB segregation (trapping) energy of hydrogen with varying the trapping density of hydrogen. The calculated GB segregation energies are shown in Fig. 4. From this figure, we can see the following.

For Fe case, hydrogen can be trapped up to about 6-7 atoms on the area of A (27.6 Å^2), because the segregation energy of "total" hydrogen atoms on A (27.6 Å^2) comes close to a minimum value and the "incremental" segregation energy of one hydrogen atom comes close to zero. For Al case, hydrogen can be trapped up to twelve atoms on the area of A (37.3 Å^2). We can see that the Al GB can trap many hydrogen atoms comparing with the Fe GB. For Cu case, hydrogen can be trapped up to six atoms on the area of A (29.2 Å^2). The segregation limit of hydrogen for Cu GB is close to that for Fe GB. However, the GB segregation energy of hydrogen atoms for Cu case is much smaller than that for Fe case. It indicates that Cu GB is difficult to trap hydrogen atoms comparing with the Fe and Al GBs.
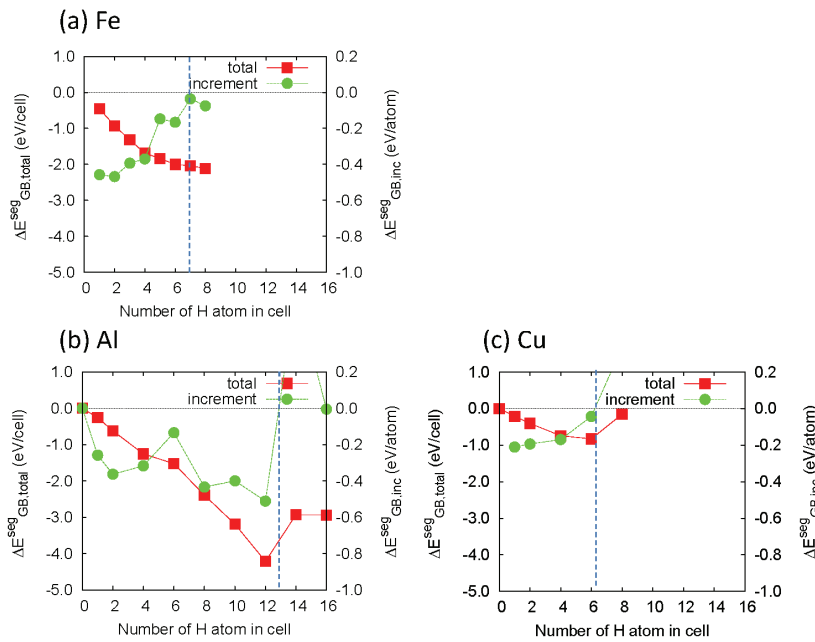

Fig. 4: Calculated grain boundary (GB) segregation (trapping) energies ($\Delta E^{seg}_{GB,total}$) of hydrogen atoms with varying trapping density for (a) bcc Fe Σ3(111) GB, (b) fcc Al Σ5(012) GB, and (c) fcc Cu Σ5(012) GB. "Total" line indicates the segregation energy for total hydrogen atoms in the grain boundary of the unit cell. The area of the GB in the unit cell is equal to A. "Increment" line indicates the incremental segregation energy per one hydrogen atom. Dashed lines roughly indicate the GB segregation limit of hydrogen atoms in the grain boundary (the area of A), where the incremental segregation energy is zero.

Thirdly, we calculated the surface segregation energy of hydrogen atoms on the bcc Fe (111) and fcc Al(Cu) (012) fracture surfaces. The calculated results are shown in Fig.5. From this figure, we can see that Fe (111) surface can trap up to six hydrogen atoms on the area of A (27.6 Å^2), Cu (012) surface can trap up to 4 hydrogen atoms on the area of A (29.2 Å^2). Al (012) surface can trap more than 8 hydrogen atoms on the area of A (37.3 Å^2).

Fourthly, we estimated the change in the cohesive energies ($2\gamma_{int}$) of bcc Fe Σ3(111) and fcc Al(Cu) Σ5(012) GBs using Eq. (1) and using the calculated results of GB and surface segregation energies as shown in Fig.4 and 5. The estimated cohesive energies are shown in Fig. 6. From this figure, we can see that the cohesive energy of GB is reduced by about 30% at most for Fe and Cu cases. However, it should be noted here that hydrogen is difficult to dissolve in fcc Cu and also difficult to be trapped at the Cu GB comparing with Fe case as stated above. For Al case, the cohesive energy of GB is reduced by about 90% at most by hydrogen segregation at GB. Although hydrogen is very difficult to dissolve in fcc Al comparing with Fe case as stated above, inner hydrogen has a very strong embrittling effect for Al GB.
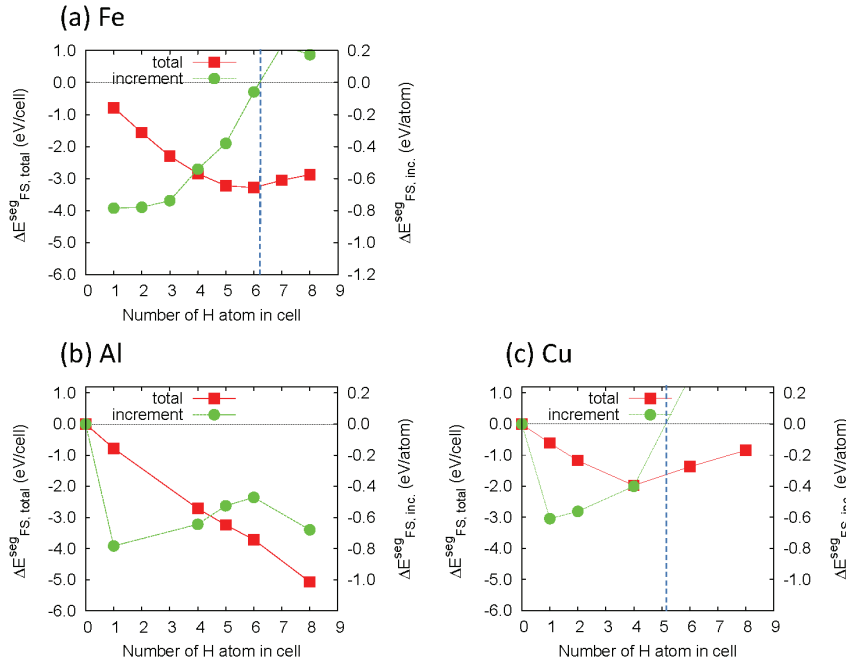
(a) Fe

(b) Al

(c) Cu

Fig. 5: Calculated surface segregation energies ($\Delta E^{seg}_{FS,total}$) of hydrogen atoms with varying segregation density for (a) bcc Fe (111) surface, (b) fcc Al (012) surface, and (c) fcc Cu (012) surface. Dashed lines roughly indicate the surface segregation limit of hydrogen atoms on the surface (the area of A), where the incremental segregation energy is zero.
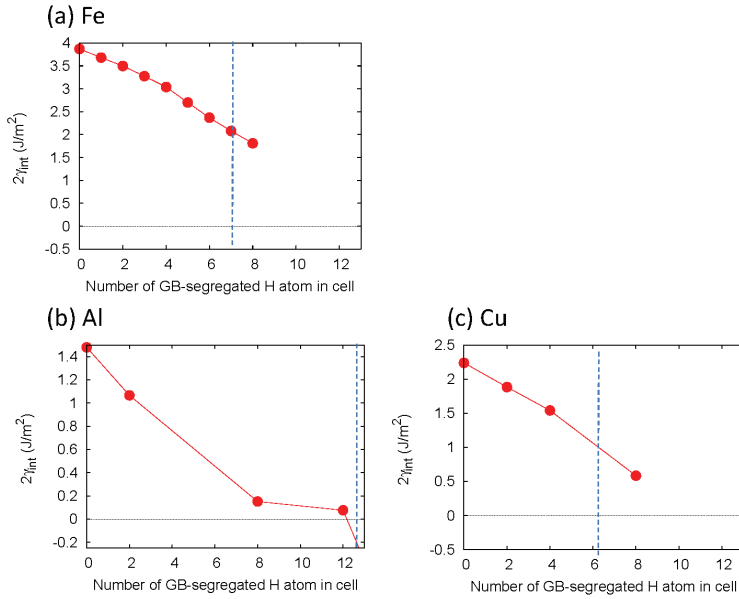
(a) Fe

(b) Al

(c) Cu

Fig.6: The change of the cohesive energy ($2\gamma_{int}$) of (a) bcc FeΣ3(111) GB, (b) fcc Al Σ5(012) GB, and (c) fcc Cu Σ5(012) GB. Dashed lines indicate the grain boundary segregation (trapping) limit of hydrogen atoms in the area of A (27.6 Å^2 for Fe, 37.3 Å^2 for Al, and 29.2 Å^2 for Cu).
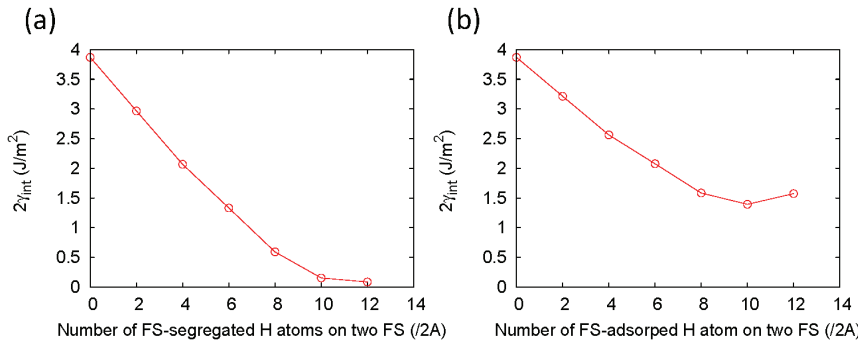
(a)

(b)

Fig. 7: The reduction of the cohesive energy $2\gamma_{int}$ of bcc Fe Σ3(111) grain boundary by the "mobile" effect of hydrogen (a) from inner bulk (solid solution state) to (111) fracture surfaces (FS), and (b) from hydrogen gas state (H_2 molecule) to (111) fracture surfaces.

In the discussions so far, the number of trapped hydrogen atoms is assumed not to change during fracture; the number of hydrogen atoms trapped at a grain boundary before fracture and that on the two fracture surfaces after fracture is assumed to be the same. However, this assumption may not be correct for the hydrogen case, because the diffusion of hydrogen is very fast even at room temperature, and the diffusion may become comparable to the crack growth velocity. For this reason, we estimated the "mobile" effect of hydrogen during fracture for bcc Fe $\Sigma 3(111)$ GB case. One possible factor is that the diffusible hydrogen atoms coming from solid solution state are trapped on the gradually formed fracture surfaces during fracture. This effect is calculated and shown in Fig. 7(a). Another possible factor is that the gasified hydrogen (H_2 molecule) in the crack opening space is adsorbed on the gradually formed fracture surfaces. This effect is also calculated and shown in Fig. 7(b). In both two cases, the cohesive energy of the grain boundary can be significantly reduced as can be seen in Fig. 7. Hereafter, we focus on the mobile effect of solid solution hydrogen.
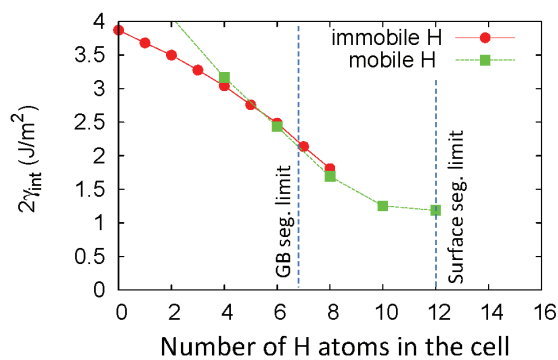

Fig.8: The reduction of the cohesive energy ($2\gamma_{int}$) of bcc Fe $\Sigma 3(111)$ GB with varying trapping (segregation) density of hydrogen atoms at GB and its two fracture surfaces. The reduction in the cohesive energy by the GB-trapped hydrogen is referred as "immobile H", which is the same as the plotting as Fig. 6(a).The reduction by the mobile effect of hydrogen that moves from solid solution state to fracture surface during fracture is referred as "mobile H", which is the same plotting as Fig. 7(a) but connected at 6 H atoms (GB seg. limit) with the line of immobile H effect.

We estimated the superposition of the "immobile" and "mobile" effects of hydrogen on the reduction of $2\gamma_{int}$ as shown in Fig. 8. In this figure, we assume that six hydrogen atoms have already trapped at the grain boundary plane (area $A = 27.6$ Å^2) of the unit cell including bcc Fe $\Sigma 3(111)$ GB, and then the mobile effect of solid solution hydrogen as shown in Fig. 7(a) is added. By the superposition of the two effects, the immobile and mobile effects of hydrogen, the cohesive energy of bcc Fe $\Sigma 3(111)$ GB is reduced by 60-70% at most as shown in Fig. 8. Recently, Wang, Akiyama, and Tsuzaki [10] have shown that the fracture stress of high strength steel was reduced by about 80 % at most with increasing diffusible hydrogen content in the slow strain rate test; the amount of fracture stress reduction is in agreement with the reduction of the cohesive energy in our calculations. In addition, Wang et al. have shown that the fracture stress reduction is saturated at 80% with increasing hydrogen content (Fig. 9 in Ref. [10]). From our calculations, this saturation can be understood to be caused by the fact that there is the density limit of hydrogen trapping on the fracture surfaces as shown in Fig. 5(a).

Here, we suggest a new idea regarding the physical origin about the upper and lower critical stresses which are observed in the constant load test of delayed fracture induced by hydrogen in high strength steels. The concept of upper and lower critical stresses are shown in Fig.1 of Ref. [11]. The upper critical stress is defined as the lowest fracture stress at which the fracture occurs without delay time. On the other hand, the lower critical stress is defined as the lowest fracture stress at which fracture occurs with very long delay time. The delayed fracture does not occur under the stress that is smaller than the lower critical stress. Looking at the calculated reduction of $2\gamma_{int}$ as shown in Fig. 8, we can find an important behavior that can explain the origin of upper and lower critical stresses. The immobile effect of hydrogen atoms that have already segregated at grain boundary reduces the grain boundary cohesive energy ($2\gamma_{int}$) by about 40% at most. In this case, the delay time for fracture is not necessary; it indicates that the upper critical stress is caused by the immobile effect of hydrogen (already trapped hydrogen atoms at the grain boundary). On the other hand, the delay time is necessary for fracture by the mobile effect of hydrogen atoms, which come from solid solution state

to the gradually formed fracture surfaces and then are trapped on the fracture surfaces. It indicates that the lower critical stress is caused by the immobile and mobile effects of hydrogen atoms. From these considerations, we suggest a new idea about the origin of the upper and lower critical stresses; *the upper critical stress is determined by the amount of immobile hydrogen atoms which are already trapped at the grain boundary before fracture, and the lower critical stress is determined by the total amount of immobile and mobile hydrogen atoms, the latter of which is additionally trapped hydrogen atoms on the gradually formed fracture surfaces during fracture coming from solid solution state or H_2 gas in the crack opening space.*

3.2 (Fe, Al, Cu)-Hg and Al-Ga systems

We performed preliminary calculations for (Fe, Al, Cu)-Hg and Al-Ga systems. We calculated the solid solution energy of Hg atom in bcc Fe and fcc Al(Cu), and that of Ga in fcc Al. Contrary to the calculations of the segregation energy in the metal-hydrogen systems, we calculated the grain-boundary and surface *adsorption* energies of liquid metal atoms. This adsorption energy is defined with reference to the solid alpha-Hg (space group No.166) or alpha-Ga (space group No.64) states. These solid states are considered to be energetically close to the liquid state, although we cannot calculate the total energy of liquid state. The calculations of the adsorption energy with varying adsorption density are future work.

The calculated results are summarized in Table 1. All the systems in this table are known to show liquid metal embrittlement experimentally [12]. From our calculated results in this table, we can see that the Hg and Ga atoms have an effect to reduce the fracture surface energy by the surface adsorption, because the surface adsorption energy is negative. It suggests that the liquid metal embrittlement can be also caused by the reduction of the surface energy, in similar to the hydrogen embrittlement as discussed in the previous subsection (3.1). Among the four systems, the Al-Ga system is considered to show a very strong embrittlement. The solid solution energy of Ga in fcc Al (0.11 eV/atom) is the smallest one, which means that Ga is easy to dissolve in fcc Al. The grain boundary adsorption energy of Ga in Al GB is also the smallest one, which means that Ga is easy to penetrate into Al GB. It is in good agreement with experimental fact [12].

Table 1: Calculated solid solution energy, grain-boundary/surface segregation energies of Hg in Fe, Al, and Cu, and those of Ga in Al. Positive solid solution energy means difficult to dissolve. Negative segregation energy means easy to segregate.

System	Solid Solution Energy (eV/atom)	Grain boundary adsorption energy, $\Delta E_{ad,atom}^{GB}$ (eV/atom)	Surface adsorption energy, $\Delta E_{ad,atom}^{FS}$ (eV/atom)
bcc Fe - Hg	2.07	0.70 in Σ3(111)GB	-0.80 on (111)FS
fcc Cu - Hg	0.63	-0.04 in Σ5(012)GB	-0.56 on (012)FS
fcc Al - Hg	0.71	0.11 in Σ5(012)GB	-0.34 on (012)FS
fcc Al - Ga	0.11	-0.06 in Σ5(012)GB	-0.35 on (012)FS

4. Conclusions

From first-principles, we calculated the grain boundary (GB) cohesive energy (work of fracture) of bcc FeΣ3(111) and fcc Al(Cu) Σ5(012) symmetrical tilt grain boundaries with varying segregation (trapping) density of hydrogen.

For Fe case, the cohesive energy is reduced by about 30% at most owing to hydrogen segregation at the grain boundary. By adding the mobile effect of hydrogen during fracture, the Fe GB cohesive energy is reduced by about 70% at most. We believe that the upper critical stress in delayed fracture

experiment is determined by the amount of hydrogen trapping at GB, and the lower critical stress is determined by the amount of hydrogen trapping at the two fracture surfaces.

For Cu case, the cohesive energy of the grain boundary of Cu is reduced by about 30% at most by hydrogen trapping in similar to Fe case. However, it is difficult for hydrogen atoms to be trapped at the Cu grain boundary, because the GB segregation energy of hydrogen atoms for Cu case is much smaller than that for Fe case. In addition, hydrogen is difficult to dissolve in Cu comparing with Fe.

For Al case, a large amount of hydrogen atoms can segregate (be trapped) at Al grain boundary compared with Fe, and the cohesive energy of Al grain boundary can be reduced by over 90% at most by inner hydrogen segregation. Contrary, gaseous (outer) hydrogen cannot decrease the fracture surface energy. These results are in good agreement with the experimental facts that inner hydrogen can cause Al grain boundary embrittlement while gaseous (outer) hydrogen cannot.

Our preliminary calculations for (Fe, Cu, Al)-Hg and Al-Ga systems show that the liquid metal (Hg and Ga) embrittlement can be caused by the same mechanism as (Fe, Cu, Al)-H systems: *the reduction of fracture surface energy*.

Acknowledgement

References

[1] M. Yamaguchi, M. Shiga, and H. Kaburaki: Science 307(2005)393-397.
[2] M. Yamaguchi, Y. Nishiyama, and H. Kaburaki: Phys. Rev. B76(2007)35418-35422.
[3] M. Yamaguchi: J. Japan Inst. Metals 72(2008)657-666. (in Japanese)
[4] M. Yamaguchi, K. Ebihara, M. Itakura, T. Kadoyoshi, T. Suzudo, and H. Kaburaki: Proceedings of Eighteenth International Symposium on Processing and Fabrication of Advanced Materials (PFAM XVIII), Sendai, Japan, 2009, Volume 1, pp. 65-74.
[5] G. Kresse and J. Hafner: Phys. Rev. B47(1993)R558-R561.
[6] G. Kresse and J. Furthmueller: Phys. Rev. B54(1996)11169-11186.
[7] G. Kresse and D. Joubert: Phys. Rev. B59(1999)1758-1775.
[8] J. R. Rice and J. –S. Wang: Mater. Sci. Eng. A107(1989)23-40.
[9] K. Ichitani and S. Osaki: Proceedings of Eighteenth International Symposium on Processing and Fabrication of Advanced Materials (PFAM XVIII), Sendai, Japan, 2009, Volume 1, pp. 55-64.
[10] M. Wang, E. Akiyama, and K. Tsuzaki: Corrosion Science 49(2007)4081-4097.
[11] A. Troiano: Trans. ASM 52(1960)54-80.
[12] M.G. Nicholas: *in Embrittlement by Liquid and Solid Metals*, Ed. by M.H. Kamdar, (The Metallurgical Society of AIME, Pennsylvania, USA, 1984) pp. 27-50.